Pulling Tethers from Adhered Vesicles

Ana-Sunčana Smith,[1] Erich Sackmann,[1] and Udo Seifert[2]
[1]*E 22 Institut für Biophysik, Technische Universität München, D-85748 Garching, Germany*
[2]*II. Institut für Theoretische Physik, Universität Stuttgart, D-70550 Stuttgart, Germany*

(Received 8 September 2003; published 21 May 2004)

The competition between adhesion and tether formation in bound vesicles is investigated. A theoretical model is developed in which tethers are induced by the application of a pulling force to the top of a strongly adhered vesicle. A critical onset force is identified where the tether spontaneously appears as part of a first order shape transition. Further growth of the tether initiates a detachment process that culminates in a continuous unbinding of the vesicle at a finite detachment force. Both critical forces, as well as all shape parameters, are calculated as a function of the reduced volume and the strength of adhesive potential.

DOI: 10.1103/PhysRevLett.92.208101 PACS numbers: 87.17.–d, 87.16.Dg, 87.80.Fe

Fluid membranes are unique among all two-dimensional elastic sheets due to their vanishing shear modulus. This property allows for spectacular deformations of these slender layers such as the formation of thin tubular structures, known as tethers. Their extraction can be realized by the application of a highly localized force, balanced against an appropriate resistance mechanism. The paradigmatic case for tether formation involves pulling on beads [1] or micropipettes irreversibly bound to a vesicle. These may serve as a means to exert axial tension [2] or as anchor points in the case of flow experiments [3].

The manipulation of tethers has been used as an investigative tool to elucidate the properties of membrane materials. In this manner, the bending modulus of bilayers [1] and the nature of the dynamic interaction of monolayers within a single bilayer [4] have been determined. Tether extraction from cells has enabled the quantification of the coupling of the cell membrane to the supporting cytoskeleton [5]. Recently, molecular motors have been employed to induce tubulation in giant vesicles [6].

Several theoretical models relevant to tether formation have appeared. The initial interest was focused on the stability of free tubes [7] and cylindrical vesicles under axial tension [8,9]. More recently, asymmetric tethered shapes have been found to result from the application of a force to the opposing poles of a vesicle [2]. In flat membranes, tether induction has been shown to rely on appropriate boundary conditions imposed at the rim of the tether [10,11], as has been verified experimentally [12].

A problem of significant biological and technological relevance is that in which the resistance mechanism to tether formation is provided by a finite adhesion potential acting on another part of the vesicle. For example, such counteraction has been used for the construction of complex networks from tethered fluid vesicles [13]. Nevertheless, a theoretical work that provides an understanding of the external adhesive counteraction to tether formation has not yet been provided. The present investigation deals with this problem and reveals a rich competition between the attractive potential and shape deformations.

Simple intuition suggests that the response of an adhered vesicle to pulling would depend strongly on the type of the adhesion achieved by the vesicle [14]. When the vesicle is bound in a *weak* potential, only part of the excess free area (resulting from the volume reduction during vesicle preparation) is used to form the adhesion plate. Pulling on such a shape causes continuous deformations, made possible by the unused excess area [15]. A *strongly* adhered vesicle should clearly undergo a different scenario. In these circumstances, the excess free area is entirely consumed by the adhesion plate so that the vesicle assumes the shape of a tense spherical cap [14]. Because of constraints on the area and volume, no deformations can be induced while maintaining a constant adhesion area. However, should sufficient force be applied to overcome the adhesive potential, a tether will be pulled out of the vesicle, initiating a detachment process. The tether can be expected to grow until the adhesion plate is spent and the detachment process is complete. In the current work, we quantitatively investigate this regime of strong adhesion. As it is safe to assume a cylindrical tether geometry [2], we consider shapes consisting of a spherical cap (a vesicle) connected to a thin tube (a tether). Variational methods are thus used to minimize the following free energy functional:

$$\mathcal{F} = \frac{\pi\kappa L}{R} - F(h + L) - WA^* + \Sigma A_{\mathrm{tot}} + PV_{\mathrm{tot}}. \quad (1)$$

The first term is the bending energy of a cylinder with radius R and length L, and is proportional to the bending rigidity κ. The variation of the bending energy of a spherical cap is an order of magnitude smaller than that of the other terms and may therefore be omitted. The second term is the energy arising from the application of a point force to the north pole of the vesicle. This energy is a function of the strength of the force ($F > 0$), and the total height (sum of the heights of the spherical cap h and the tether). The next term is the adhesion energy associated with a given contact potential, of strength $W > 0$, and is proportional to the area of the adhered surface A^*. The last two terms in Eq. (1) emerge from constraints imposed to maintain constant total area ($A_{\rm tot}$) and volume ($V_{\rm tot}$), by adjusting the Lagrange multipliers for the tension (Σ) and pressure (P), respectively.

The results are presented in reduced units, scaled by the area of a unit sphere $A_s = 4\pi R_s^2$, and $R_s = 1$. Hence p, σ, w, v, and f become dimensionless parameters, and are defined as $p = PR_s^3/\kappa$, $\sigma = \Sigma R_s^2/\kappa$, $w = WR_s^2/\kappa$, $v = 3V_{\rm tot}/(4R_s^3\pi)$, and $f = FR_s/(\pi\kappa)$. In addition, $A_{\rm tot} = A_s$. For a vesicle of radius of $R = 10$ μm and bending modulus $\kappa = 10^{-19}$ J, one unit of force f is equal to 0.3 pN, and one unit of adhesion strength w is 10^{-7} J m^{-2}.

To find stationary solutions of the free energy functional, the first variation with respect to all shape parameters (A^*, h, L, and R) is performed. The obtained relations are then solved simultaneously with the constraints on the total volume and area, for a given set of v, w, and f. Physically relevant solutions are those that are real and have values of all shape parameters greater than zero (in addition, the tether radius must be smaller than the radius of the spherical cap). Generally, there exist two solutions that satisfy these requirements for a given set of parameters. The shape associated with the lower total energy is considered to be locally stable and is thus the relevant one in the following discussion. Examples of the calculated shapes are presented in Fig. 1.

Phase diagram.—The phase diagram can be presented for either constant v (left panel of Fig. 2) or constant w (right panel). In both cases, three regions can be observed. Most prominent is the region shaded in gray, where stable solutions are tethered vesicles. This region is open in the $f - w$ diagram as there is no theoretical upper limit to the strength of the adhesion potential. As the reduced volume of the vesicle must be in the range $0 < v \leq 1$, the entire phase space (for fixed w) is presented in the $f - v$ diagram. The lower boundary of the gray regions is congruous with the onset of tether formation (denoted as f_o) and is a line of a first order shape transition. For forces below this line, the shape of a tetherless spherical cap is a stable solution. The upper boundary of the regions where tethers are stable (denoted as f_d) corresponds to forces at which the tethered vesicle detaches from the surface with the adhesion area $A^* \rightarrow 0$ when $f \rightarrow f_d$. As detachment is a continuous process, this boundary is a line of a second order shape transition. Above this line, the stable solution corresponds to a free vesicle far away from the substrate.

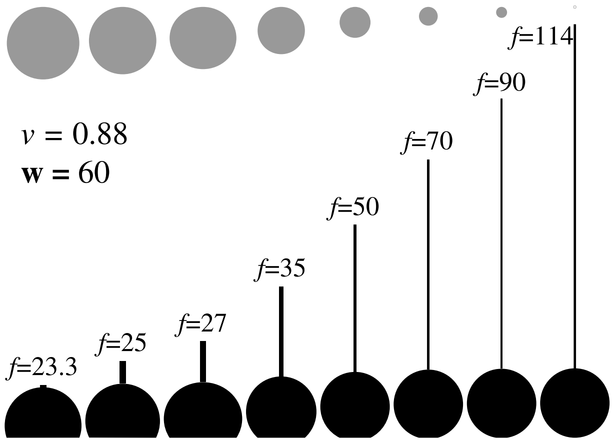

FIG. 1. An adiabatic force load initiates a detachment process. Finite forces are found for both the tether onset ($f_o \simeq 23.3$) and the vesicle detachment ($f_d \simeq 114$). Shapes of tethered vesicles are presented for different forces in black. Gradual but total loss of the adhesion area (top, gray circles) can be observed as the tether length increases.

Tethered shapes.—The calculation of shapes, by minimizing Eq. (1) subject to constraints, results in algebraic expressions for all variables. Because of the complexity of these equations, they will not be presented here in their full form. However, it is possible, by assuming that the volume of the tether is much smaller than the volume of the vesicle, to obtain an expression for the tether length as a function of force:

$$L \simeq (1 - v^{2/3})f. \tag{2}$$

This approximate relationship assumes the role of an asymptote at large forces and adhesion strengths (see Fig. 3). For small w, the exact solution is nonlinear in the whole range of applicable forces and the approximate solution defined by Eq. (2) is reached only at the detachment point. For larger adhesion strengths, the linear dependency of the tether length on the applied force is in good agreement with the exact solution, for the majority of feasible forces. This result predicts that, for smaller values of v, the tether length grows faster with the force. Nevertheless, for a fixed volume, very similar solutions for the tether length are obtained for very different w. As an application of Eq. (2) the linear regime of tether retraction from Fig. 5 of Ref. [13] has been fitted and resulted in a reduced vesicle volume of $v = 0.93 \pm 0.02$.

Extracting the leading terms from the exact solutions (not presented) leads to well known results for the tether

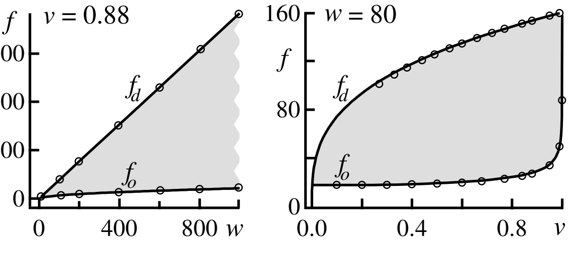

FIG. 2. Examples of $f - w$ (left) and $f - v$ (right) phase diagrams. Regions of locally stable tethered shapes are indicated in gray. The line associated with f_o is the boundary between regions of stable tethered shapes and stable shapes consisting of a bound spherical cap. The f_d line belongs to continuous unbinding transitions from bound tethered shapes to free vesicles. Approximate solutions (lines) from Eqs. (4) and (5) and the exact solutions (circles) are shown.

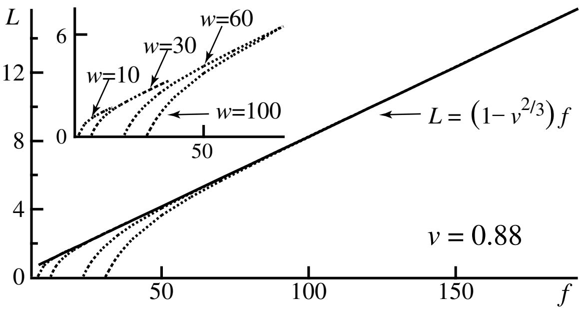

FIG. 3. The length of a tether as a function of force for different adhesion strengths. The approximate solution (thick line) is overlaid with exact solutions (dotted lines).

radius and tension:

$$R \approx \frac{2}{f}, \qquad \sigma \approx \frac{f^2}{8}. \tag{3}$$

These relationships have already been derived and verified experimentally [1,8], for the special case of a tether extracted from a vesicle partially drawn into a pipette. Now, however, these results are obtained as part of a more general model, which includes a finite adhesion strength. As was the case for the tether length, these expressions will become exact in the limit of large f and w (and $f/w =$ const). Inspection of Fig. 4, where the approximate result is compared to the exact solution, clearly demonstrates this limit.

Within the current model, shapes with arbitrarily high tensions can be calculated, but their existence is limited by the lysis tension of the membrane ($\Sigma_l \approx 10^{-3}$ N m^{-1}). Once such tension is exceeded, the tether will rupture. Using Eq. (3), it is easy to estimate the lysis point force to be $F_l \approx 90$ pN for a membrane with $\kappa = 25kT$. Interestingly, the approximate solutions obtained for R and σ, are not sensitive to the adhesion strength or the reduced volume. Consequently, for any value of the applied force ($f_o < f < f_d$), almost identical solutions can be found for quite different values of v and w. This can be seen in Fig. 4, where the intervals of stable solutions belonging to different w overlap. It is therefore important to define the boundaries of the interval where tethered shapes exist as a function of state variables (v and w). This will be discussed in the following sections.

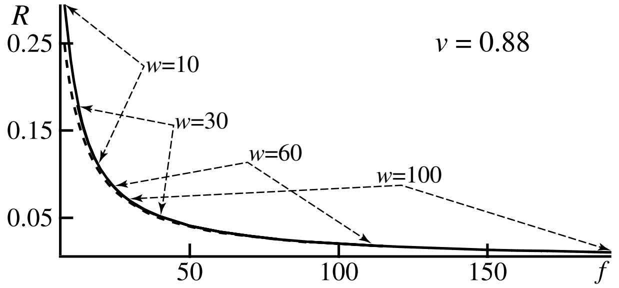

FIG. 4. The tether radius as a function of force for different adhesion strengths. The exact solution (thick line) is rapidly approached by the approximate one (dotted line). The broken arrows indicate the regions where stable solutions are found for a particular adhesion strength.

Onset of tether formation.—The conditions for tether appearance can be determined by setting R and L to zero. In this case, the constraints on the area and volume of the vesicle with no tether are sufficient to determine the characteristics of the spherical cap (h and A^*). The shape obtained in this way is identical to the one arising from the variation of the free energy at $f = 0$. It is the spherical cap of minimum height h_o (see Fig. 5) and maximum adhesion area ($A_o^* = 2 - h_o^2/2$). Because of strong adhesion, this shape is a function of only the reduced volume and is not dependent on the adhesion strength. At the onset of tether formation, the tension must approach that given in Eq. (3). This may be used to derive the approximate onset force [$f_o = f_o(v, w)$] and pressure [$p_o = p_o(v, w)$]:

$$f_o \simeq \frac{-h_o + \sqrt{h_o^2 + A_o^{*^2} + A_o^* h_o^2 w}}{0.5A_o^*}, \qquad p_o \simeq \frac{4w - f_o^2}{2h_o}. \tag{4}$$

The comparison of this force with the exact solution is presented in the phase diagram (see Fig. 2, both panels). Excellent agreement is obtained for the whole range of adhesion strengths and reduced volumes. As the height of the vesicle (h_o) and the size of the adhesion plate (A_o^*) are independent of the adhesion strength, the onset line (f_o) in the left panel of Fig. 2 is proportional to $\sqrt{w}$. This analysis infers that for all $f < f_o$, the spherical cap parametrized with h_o and A_o^* is a stationary stable solution. A force load will merely adjust the tension and the pressure until the tether emerges at $f = f_o$.

In the *limit* of strong adhesion ($w \rightarrow \infty$) this scenario is exact. However, in the *regime* of strong adhesion ($w \gg 1$), the very small amounts of excess area that remain free upon adhesion could allow for continuous (but slight)

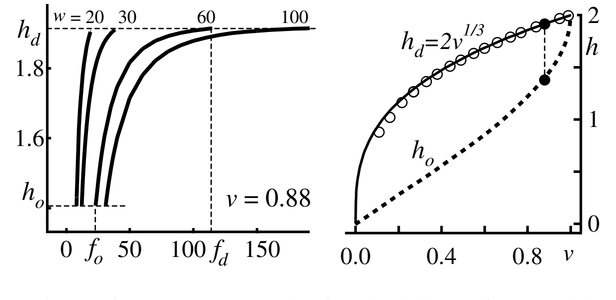

FIG. 5. Left: The exact results for the height of the vesicle as a function of force for different adhesion strengths (thick lines). Approximate onset and detachment heights (all w) and forces ($w = 60$) are indicated. Right: The exact onset heights (dotted line) and a comparison of approximate (thin line) and exact (empty circles) solutions for the detachment height as a function of reduced volume. Exact solutions are calculated with $w = 80$. The filled circles indicate solutions for $v = 0.88$.

vesicle deformations at forces close to the zero force. Within the current model, these shapes are mapped onto the spherical cap at $f = 0$ and should not affect the discontinuous nature of the shape transition. The appearance of such a transition is a consequence of both the applied constraints and the adhesion strength. Hence, it is not surprising that models for tether formation [10,11], which lack an equivalent of adhesion to provide a counteractive contribution to the free energy (and are in a different geometry), find a continuous transition.

Detachment.—A critical detachment force (f_d), corresponding to zero adhesion area ($A_d^* = 0$), can be calculated by assuming that the volume of the tether is much smaller than the volume of the vesicle. In this case $h \rightarrow 2v^{1/3}$ when $A^* \rightarrow 0$. The validity of this assumption can be confirmed by the inspection of Fig. 5. For constant reduced volume (left panel), the asymptotic detachment height ($h_d \approx 2v^{1/3}$) is reached independently of the adhesion strength. For a constant adhesive potential (right panel), very good agreement between the asymptotic and the exact solutions is obtained. However, discrepancies emerge for small values of v, implying that the chosen w ($w = 80$) acts as a strongly adhesive potential for large values of the reduced volume, but is relatively weak for very deflated vesicles ($v < 0.35$). Indeed, as w increases, the agreement between the approximate and exact solution improves for small v. Minimizing the free energy using the expression for h_d leads to an approximate relationship for the detachment force:

$$f_d \approx 2v^{1/3}w. \tag{5}$$

This equation is plotted in the aforementioned phase diagrams (Fig. 2). For constant volume (left panel), the linear dependence of f_d on the adhesion strength is confirmed. In the diagram for constant w (right panel), f_d obeys the inverse cubic dependence on the reduced volume. The discrepancies for small volume between the full algebraic solution and the approximate one share the same origin as those discussed above for the detachment height. When the expression for f_d is combined with Eqs. (2) and (3), the remaining detachment variables emerge as functions of only the state parameters v and w:

$$\begin{aligned} R_d &\approx v^{-1/3}w^{-1}, \qquad & L_d &\approx 2(v^{1/3} - v)w, \\ \sigma_d &\approx \tfrac{1}{2}v^{2/3}w^2, \qquad & p_d &\approx -v^{1/3}w^2. \end{aligned} \tag{6}$$

Closer inspection reveals that the obtained detachment pressure and tension satisfy the Laplace equation.

Summarizing perspective.—Applying a pointlike force to a strongly bound vesicle leads to tether formation for a range of forces intermediate between the onset and detachment values. These two critical forces are uniquely determined by the experimentally relevant variables, w and v. Together with good estimates of the tether length and radius, this model should provide an experimentally useful tool to quantitatively probe the adhesion strength by monitoring the geometrical properties of the tether.

An important future ramification of this model will allow for discrete binding sites. In this case, the effective strength of adhesion may vary during a force load, due to the exchange of mobile receptors between the bound and free parts of the membrane. Therefore, during the detachment process, the plain applicability of the current results is not obvious. However, at the very least, average adhesion strengths, for both the onset and detachment points, should be obtainable from the presented model.

The conclusions outlined herein arise because of the competition between adhesion and tether formation. As such, a similar treatment should be applicable to arbitrary tether positions. In this way, the stability of lipid nanotube-vesicle networks [13] could well be understood following the reasoning presented in this Letter.

This work has been supported by Deutsche Forschungsgesellschaft through SFB 563. A.- S.S. gratefully acknowledges the Department of Applied Mathematics at the ANU, Canberra, Australia, for hospitality.

[1] L. Bo and R. E. Waugh, Biophys. J. **55**, 509 (1989); R. E. Waugh and R. M. Hochmuth, Biophys. J. **52**, 391 (1987); V. Heinrich and R. E. Waugh, Ann. Biomed. Eng. **24**, 595 (1996).

[2] V. Heinrich *et al.*, Biophys. J. **76**, 2056 (1999).

[3] O. Rossier *et al.*, Langmuir **19**, 575 (2003).

[4] E. Evans and A. Yeung, Chem. Phys. Lipids **73**, 39 (1994).

[5] D.V. Zhelev and R. M. Hochmuth, Biophys. J. **68**, 2004 (1995); R. M. Hochmuth and W. D. Marcus, Biophys. J. **82**, 2964 (2002).

[6] A. Roux *et al.*, Proc. Natl. Acad. Sci. U.S.A. **99**, 5394 (2002).

[7] H. J. Deuling and W. Helfrich, Blood Cells **3**, 713 (1977); Z.-C. Ou-Yang and W. Helfrich, Phys. Rev. A **39**, 5280 (1989).

[8] D. J. Bukman, J. H. Yao, and M. Wortis, Phys. Rev. E **54**, 5463 (1996).

[9] B. Božič *et al.*, Biophys. J. **61**, 963 (1992); B. Božič, S. Svetina, and B. Žekš, Phys. Rev. E **55**, 5834 (1997).

[10] T. R. Powers, G. Huber, and R. E. Goldstein, Phys. Rev. E **65**, 041901 (2002).

[11] I. Derényi , F. Jülicher, and J. Prost, Phys. Rev. Lett. **88**, 238101 (2002).

[12] N. Maeda, T. J. Senden, and J.-M. di Meglio, Biochim. Biophys. Acta **1564**, 165 (2002).

[13] M. Karlsson *et al.*, Proc. Natl. Acad. Sci. U.S.A. **99**, 11573 (2002).

[14] U. Seifert and R. Lipowsky, Phys. Rev. A **42**, 4768 (1990).

[15] A.-S. Smith, E. Sackmann, and U. Seifert, Europhys. Lett. **64**, 281 (2003).